

SVM-based Identification and Un-calibrated Visual Servoing for Micro-manipulation

Xin-Han Huang Xiang-Jin Zeng Min Wang

Department of Control Science and Engineering, Huazhong University of Science and Technology, Wuhan 430074, PRC

Abstract: This paper presents an improved support vector machine (SVM) algorithm, which employs invariant moments-based edge extraction to obtain feature attribute. A heuristic attribute reduction algorithm based on rough set's discernible matrix is proposed to identify and classify micro-targets. To avoid the complicated calibration for intrinsic parameters of camera, an improved Broyden's method is proposed to estimate the image Jacobian matrix which employs Chebyshev polynomial to construct a cost function to approximate the optimization value. Finally, a visual controller is designed for a robotic micromanipulation system. The experiment results of micro-parts assembly show that the proposed methods and algorithms are effective and feasible.

Keywords: Micro-assembly, support vector machine, part identification, Broyden method, visual servoing.

1 Introduction

Micro-robot has a wide range of applications in micro-electromechanical systems. In order to assemble multi micro objects, it is necessary to identify these objects first. In the pattern recognition field, the moment feature is used as one of the shape features extensively. Invariant moments are the statistical properties of images which are invariant to translation, reduction, and rotation. Hu^[1] firstly used invariant moments for regional shape recognition. Because the moment feature cannot be calculated directly in close or open structure, it needs to construct regional structure first. Besides, the moment is involved in the calculation of all the pixels of intra-regional and border, so it is time-consuming. In this paper, we propose an edge extraction algorithm to process image first and then calculate the edge image's invariant moments to obtain the feature attribute, which solves the problems mentioned above.

After feature attribute extraction, the classification algorithm should be provided for the final target identification. There are mainly three kinds of classifiers. The first is the statistics-based method such as Bayesian method, K-nearest neighbors (KNN) method, support vector machine (SVM), and so on^[2-7]. The second is the rule-based method such as decision tree and rough sets. The last one is the artificial neural network method. SVM algorithm is a solution to convex optimization problems, and it is better than others because its local optimal solution is definitely the global optimal solution. Therefore, we employ SVM to classify the targets. However, the classic SVM algorithm is established on the basis of the quadratic planning. It cannot distinguish the attribute importance through training sample set. Also, it is time-consuming for large volume data classification and time series prediction. It must shorten the training time and reduce the occupied space of the training sample set to satisfy real-time data processing.

For the problems mentioned above, an improved support vector machine classification algorithm is proposed to apply edge extraction's invariant moments for obtaining object's feature attribute^[8]. In order to enhance operation effectiveness and improve classification performance, a rough-set-based feature attribute reduction algorithm has been developed to distinguish the importance of training data set^[9,10].

In order to meet highly precise micro-manipulation task, a robot must employ visual servoing methods. Usually, visual servoing needs to calibrate precisely the intrinsic parameter of the camera. However, system calibration is a complicated and difficult problem, especially for micro-manipulation based on microscope vision. Therefore, we present an online uncalibrated method to estimate the image Jacobian matrix.

Previous researches^[11-13] developed online estimation methods for image Jacobian matrix. Piepmeier et al.^[14,15] proposed a moving target tracking task based on the quasi-Newton optimization method. This approach is adaptive, but cannot guarantee the stability of visual servoing. Malis's^[16] method can keep the parameters of vision servo controller constant when the intrinsic parameter of camera is changed. Su et al.^[17] presented a motion 3-dimensional object tracking method based on global vision feedback.

Unfortunately, the current estimation methods have some problems, such as estimation lag, singularity and low convergence speed. Especially in dynamic circumstances, those problems become more serious^[18]. To deal with those problems, we use a Broyden's method to estimate the image Jacobian matrix. The method employs Chebyshev polynomial to construct a cost function which approximates the optimization value and improves the convergence of estimation.

To verify the effectiveness of the methods, a proportional-derivative (PD) visual controller with estimated Jacobian matrix is used to make the feature converge for satisfactory dynamic performance. The micro-assembly robot experiments confirm that the proposed method is effective and

Manuscript received March 5, 2009; revised May 25, 2009
This work was supported by National Natural Science Foundation of China (No. 60873032) and National High Technology Research and Development Program of China (863 Program) (No. 2008AA8041302)

feasible.

2 Objects identification

2.1 Invariant moments theory

Assume that $f(i, j)$ represents a two-dimensional continuous function. Then, its $(p + q)$ th-order moments can be written as follows:

$$M_{pq} = \int \int i^p j^q f(i, j) di dj, \quad p, q = 0, 1, 2, \dots \quad (1)$$

In terms of image computation, we generally use the sum formula of the $(p + q)$ th-order moments shown as follows:

$$M_{pq} = \sum_{i=1}^M \sum_{j=1}^N f(i, j) i^p j^q, \quad p, q = 0, 1, 2, \dots \quad (2)$$

where p and q can choose the entire non-negative integer, and they create infinite sets of the moments. According to Papulisi's theorem, the infinite sets can determine completely two-dimensional image $f(i, j)$.

In order to ensure local invariance of the shape feature, we must compute the image $(p + q)$ th-order center moment, that is, to calculate the invariant moments using the center of object as the origin of the image. The center of object (i', j') can be obtained from zero-order moment and first-order moment. The centre-moment formula can be shown as follows:

$$M_{pq} = \sum_{i=1}^M \sum_{j=1}^N f(i, j) (i - i')^p (j - j')^q, \quad p, q = 0, 1, 2, \dots \quad (3)$$

At present, most studies about the two-dimensional invariant moments focus on extracting the moment from the full image. This will increase the computation and impact on the real-time system. Therefore, we propose an invariant moment method based on edge extraction which gets the edge image first and then obtains the invariant moment feature attributes. Obviously, this method keeps the region feature of moment and reduces the computation greatly.

The formulas of the seven invariant moments are shown in (4), which can meet the invariance of the translation, rotation and scale.

$$\begin{aligned} \Phi_1 &= m_{20} + m_{02} \\ \Phi_2 &= (m_{20} - m_{02})^2 + 4m_{11} \\ \Phi_3 &= (m_{30} - 3m_{12})^2 + (3m_{21} - m_{03})^2 \\ \Phi_4 &= (m_{30} + m_{12})^2 + (m_{21} + m_{03})^2 \\ \Phi_5 &= (m_{30} - 3m_{12})^2 (m_{30} + m_{12}) [(m_{30} + m_{12})^2 - \\ &\quad 3(m_{21} + m_{03})^2] + (3m_{21} - m_{03})(m_{21} - m_{03}) \cdot \\ &\quad [3(m_{30} + m_{12})^2 - (m_{21} + m_{03})^2] \\ \Phi_6 &= (m_{20} - m_{02}) [(m_{30} + m_{12})^2 - 3(m_{21} + m_{03})^2] + \\ &\quad 4m_{11}(m_{30} + m_{12})(m_{21} + m_{03}) \\ \Phi_7 &= (3m_{12} - m_{30})^2 (m_{30} + m_{12}) [(m_{30} + m_{12})^2 - \\ &\quad 3(m_{21} + m_{03})^2] - (m_{03} - 3m_{21}) [3(m_{30} + m_{12})^2 - \\ &\quad (m_{21} + m_{03})^2]. \end{aligned} \quad (4)$$

2.2 Improved support vector machine

2.2.1 Support vector machine

The basic idea of SVM is to apply a nonlinear mapping Φ to map the data of input space into a higher-dimensional feature space, and then implement the linear classification in this higher-dimensional space.

Assume that the sample set (x_i, y_i) , $(i = 1, \dots, n)$, $x \in R_d$ can be separated linearly, where x is a d dimensional feature vector, and $y \in \{-1, 1\}$ is the class label. The general form of judgment function in its linear space is $f(x) = w \cdot x + b$. Then, the classification hyper plane equation is

$$w \cdot x + b = 0. \quad (5)$$

If classes m and n can be separated linearly in the set, then there exists (w, b) to meet

$$\begin{aligned} w \cdot x_i + b &> 0, & x_i \in m \\ w \cdot x_i + b &< 0, & x_i \in n \end{aligned} \quad (6)$$

where w is the weight vector, and b is the classification threshold. According to (5), if w and b are zoomed in or out at the same time, the classification hyper plane in (5) will keep invariant. We presume that all sample data meet $|f(x)| \geq 1$, and that the samples that are closest to classification hyper plane meet $|f(x)| = 1$. Then, this classification gap is equivalent to $2/\|w\|$. Thus, the classification gap is biggest when $\|w\|$ is minimum.

2.2.2 Improved support vector machine

For the completion of the sample training, it is a usual method that all the normalization feature attribute values are used for modeling, which will inevitably increase the computation and may lead to the misjudgment of the classification system for some unnecessary feature attributes. Therefore, proposing a judgment method to distinguish the attribute importance is necessary. First, we use rough set theory to complete the judgment for samples attribute's importance and then carry out an improved SVM to forecast classification based on the reduction attributes.

2.2.3 Rough set theory^[19,20]

Presume that a decision-making system is $S = (U, A, V, f)$, where U is the domain with a non-null limited set and $A = C \cup D$. C and D represent conditions and decision-making attributes set, respectively. V is the range set of attributes ($V = \bigcup_{a \in A} V_a$), and V_a is the range of attribute a . f is information function ($f : UX A \rightarrow V$). If there exists $f(x, a) \in V_a$ under $\forall x \in U$ and $a \in A$, and $\forall B \subseteq A$ is a subset of the conditions attributes set, then we call $\text{ind}(B)$ to be un-distinguish relationship of S . Formula $\text{ind}(B) = \{(x, y) \in UXU | \forall a \in B, f(x, a) = f(y, a)\}$ represents that x and y are indivisible under subset B . Given $X \subseteq U$, $B(x_i)$ is the equivalent category, including x_i in terms of the equivalent relationship $\text{ind}(B)$. We can define the next approximate set $\underline{B(X)}$ and the last approximate set $\overline{B(X)}$ of subset X as follows:

$$\underline{B(X)} = \{x_i \in U | B(x_i) \subseteq X\}$$

$$\overline{B(X)} = \{x_i \in U | B(x_i) \cap X \neq \emptyset\}.$$

If there is $\overline{B(X)} - B(X) = \emptyset$, the set X is able to define a set based on B . Otherwise, call X the rough set based on B . The positive domain of X based on B is the object set that can be determined to belong to X -based knowledge B , i.e., $POS_B(X) = \overline{B(X)}$. The dependence of decision-making attributes D and conditions attributes C can be defined as follows:

$$\gamma(C, D) = \frac{\text{card}(POS_C(D))}{\text{card}(U)}$$

where $\text{card}(X)$ is the base number of the set X .

The attributes reduction of rough set is that the redundant attributes are deleted without losing information. The formula $R = \{R | R \subseteq C, \gamma(R, D) = \gamma(C, D)\}$ is the reduction attributes set. Therefore, we can use equation attributes dependence as a condition for terminating iterative computing.

In order to complete the attribute reduction, we propose a heuristic attribute reduction algorithm based on rough set's discernible matrix, which uses the frequency at which attributes occur in matrix as the heuristic rules and then obtains the minimum attributes relative reduction.

The discernible matrix was introduced by Skowron and Rauszer^[21] and has been defined as

$$(c_{ij}) = \begin{cases} a \in A : r(x_i) \neq r(x_j), & D(x_i) \neq D(x_j) \\ \emptyset, & D(x_i) = D(x_j) \\ -1, & \forall r, \exists r(x_i) = r(x_j), \\ & D(x_i) \neq D(x_j). \end{cases} \quad (7)$$

According to (7), the values of elements are the different attributes combination when the attributes for the decision-making are different and the attributes for the conditions are different. The values of elements are null when the attributes for the decision-making are the same. The values of elements are -1 when the attributes for the decision-making are the same and the attributes for the conditions are different.

If $p(a)$ is the attribute importance formula of attribute a , we can propose the following formula according to the frequency at which attribute occurs.

$$p(a) = \gamma \frac{1}{|U^2|} \sum_{a \in c_{ij}} \frac{1}{|c_{ij}|} \quad (8)$$

where γ is the general parameter, and c_{ij} are the elements of the discernible matrix. Obviously, the greater the frequency at which attribute occurs, the greater its importance. Therefore, we can compute the importance of attributes using the heuristic rules in (8) and eliminate the attribute whose importance is the smallest. Then, the relative reduction of attributes can be obtained. After the attributes have been reduced, the sample feature attributes will be sent to SVM to establish the model. Finally, we can finish the classification of the final prediction data.

Input. The decision-making table $(U, A \cup D, V, f)$

Output. The relative attribute reduction

Algorithm steps:

Step 1. Compute the identification discernible matrix M .

Step 2. Determine the core attributes and find the attributes combination that the core attributes do not include.

Step 3. Obtain conjunctive normal form $P = \wedge(\vee c_{ij} : (i = 1, 2, 3, \dots, s; j = 1, 2, 3, \dots, m))$ of the attributes combination by Step 2, where c_{ij} are elements of each attribute combination. Then, convert the conjunctive normal form to disjunctive normal form.

Step 4. Determine the importance of attribute according to (8).

Step 5. Compute the smallest importance of attribute by Step 4 and then eliminate the attribute to obtain the attributes reduction.

3 Jacobian matrix estimation

3.1 Image Jacobian

The image Jacobian matrix J_q is defined as

$$\dot{f} = J_q(q)\dot{q} \quad (9)$$

i.e.,

$$J_a(q) = \left[\frac{\partial f}{\partial q} \right] = \begin{bmatrix} \frac{\partial f_1(q)}{\partial q_1} & \dots & \frac{\partial f_1(q)}{\partial q_m} \\ \vdots & & \vdots \\ \frac{\partial f_n(q)}{\partial q_1} & \dots & \frac{\partial f_n(q)}{\partial q_m} \end{bmatrix} \quad (10)$$

where $q = [q_1, q_2, \dots, q_m]^T$ represents the coordinates of robot end-effector in the task space, and $f = [f_1, f_2, \dots, f_n]^T$ is the corresponding position in image feature.

3.2 Broyden based Jacobian matrix estimation

The image Jacobian matrix can be calculated by calibrating the inner and outer parameters of robotic system and sensor system. However, it is impossible to obtain precise system parameters under a dynamic or uncertain environment. Therefore, we employ Broyden's method to estimate the image Jacobian matrix.

The Broyden nonlinear equation is

$$A_{k+1} = A_k + \frac{(y^{(k)} - A_k s^{(k)})s^{(k)T}}{\|s^{(k)}\|_2^2}, \quad k = 0, 1, \dots \quad (11)$$

Apply the Broyden method to construct the estimation model of image Jacobian matrix. According to (1), the feature error of two images is represented as

$$e_f(q) = f^d - f^c \quad (12)$$

where f^d is the feature of the expectation image, and f^c is the feature of the current image. The Taylor series expansion of e_f is shown as

$$e_f(q) = e_f(q_m) + \frac{\partial e(q_m)}{\partial q}(q - q_m) + \dots + R_n(x) \quad (13)$$

where $R_n(x)$ is Lagrange remains.

Define $J_q^*(q_n)$ as the N -th image Jacobian to be estimated.

$$J_q^*(q) = \frac{\partial e(q_n)}{\partial q}. \quad (14)$$

By ignoring the high-order term and Lagrange remains $R_n(x)$, the following equation can be obtained from (13) and (14):

$$e_f(q) = e_f(q_m) + J_q^*(q_n)(q - q_m). \quad (15)$$

If counterpoints of J , Δe , and Δq are A , y , and s , respectively we can construct the image Jacobian estimation model based on Broyden as follows:

$$J_q^*(q_{k+1}) = J_q^*(q_k) + \frac{(\Delta e - J_q^*(q_k)\Delta q)\Delta q^T}{\Delta q^T \Delta q}. \quad (16)$$

The Broyden algorithm estimates the optimization value by employing iterative computation. Therefore, it needs the end condition of iterative computation. We employ Chebyshev polynomial to construct the cost function to approximate the optimization value in the next session.

3.3 Cost function with Chebyshev polynomial

Given

$$N_K(q) = e_f(q_k) + J_q^*(q)(q - q_k) \quad (17)$$

if $N_k(q) \in [-1, 1]$, for Chebyshev polynomial serial $\{T_n, n = 0, 1, \dots\}$ with weight $\rho(x) = (1 - x^2)^{-1/2}$, its optimization square approximation polynomial is

$$s_n^*(x) = \frac{a_0}{2} + \sum_{i=1}^n a_i T_i(x) \quad (18)$$

where

$$a_i = \frac{2}{\pi} \int_{-1}^1 \frac{N_k(x)T_i(x)}{\sqrt{1-x^2}} dx, \quad i = 0, 1, \dots, n. \quad (19)$$

Then,

$$N(q) = \lim_{n \rightarrow \infty} \left(\frac{a_0}{2} + \sum_{i=1}^n a_i T_i(q) \right). \quad (20)$$

Usually, $N_k(q) \in [a, b]$. We must convert $[a, b]$ into $[-1, 1]$. The following equation can finish the convert.

$$t = \frac{b-a}{2}x + \frac{b+a}{2}. \quad (21)$$

If we use part sum s_n^* as $N(q)$ approximation, under some conditions, there is a fast speed for $a_n \rightarrow 0$.

3.4 Chebyshev polynomial approximation

Piepmeyer et al.^[14,15] provided recursion least square (RLS) algorithm to approximate the best value for minimum cost function, which is shown as

$$\min(k) = \sum_{i=1}^n \lambda^{k-i} \|N_k(q_{i-1}) - N_{i-1}(q_{i-1})\|^2 \quad (22)$$

where λ is the rate of dependency of the prior data.

In order to obtain the performance, the cost function using RLS algorithm depends on the data of several previous steps. This means that the prior knowledge must be obtained for finishing the task. Similarly, the cost function with Chebyshev polynomial is

$$M(k) = \sum_{i=1}^n \|N_k(q_{i-1}) - N_{i-1}(q_{i-1})\|^2. \quad (23)$$

It is clear that the cost function using Chebyshev polynomial is independent of the prior data.

3.5 Jacobian estimator

A Broyden estimator of image Jacobian with Chebyshev polynomial approximate algorithm is developed. A graphical representation of the estimate process is shown in Fig. 1.

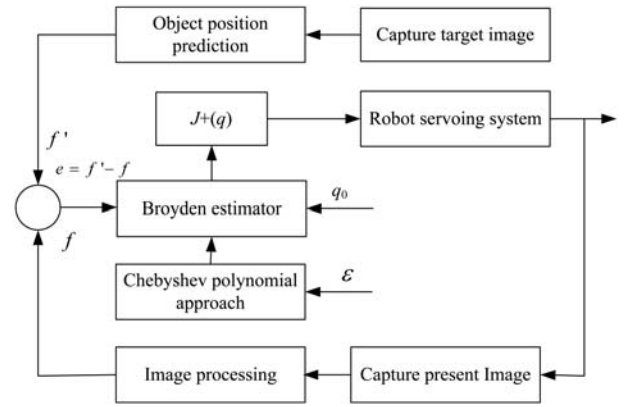


Fig. 1 A Broyden estimator of image Jacobian with Chebyshev polynomial approximate algorithm

Firstly, the Broyden estimator starts with initial end effector position q^0 and precision ε . Then, the camera captures an image of end effector for extracting corresponding image coordinate feature f^k , which provides the possibility for calculating $J^*(q^k)$ according to formula $J^*(q^k) = [f'(q^k)]^{-1}$. Secondly, the camera captures an image of target to obtain expectative image coordinate feature f^{k+1} . With the obtained $J^*(q^k)$, the servoing control law can be deduced in the section of the vision controller design. Finally, program judges whether precision ε meets system requirement or not. If precision ε meets the requirement, the program will end; otherwise, the system will execute repeated processing.

4 Design of visual controller

In order to finish positioning task of three-dimensional micro-objects, in the practical operation, micro-manipulation tasks will be divided into horizontal direction (X - Y plane) movement and vertical direction (Z -axis) movement. The manipulator moves in the X - Y plane and locates micro-parts first, then makes movements in the Z -axis vertically and locates micro-parts at the centre. Therefore, we can compute horizontal and vertical image Jacobian matrix, which can complete locating and tracking three-dimensional objects.

The changes of robotic movement $[dx, dy]^T$ and image characteristics $[du, dv]^T$ can be written as follows.

$$\begin{bmatrix} dx \\ dy \end{bmatrix} = J \begin{bmatrix} du \\ dv \end{bmatrix}. \quad (24)$$

According to the online estimation of image Jacobian matrix J based on Broyden method, we can set the position of the error $e = f^d - f^c$, where f^d is the expectation of the object position (600 μm diameter cylindrical parts), and f^c is the centre position of the end effector. Then, the control law of PD controller $u(k)$ is

$$u(k) = K_p(j^T J)^{-1} j^T e(k) + K_d(j^T J)^{-1} j^T \frac{\Delta e(k)}{T_s} \quad (25)$$

where T_s is the time interval, K_p is the proportional gain, and K_d is the differential gain.

5 Experiments

Fig. 2 shows an experiment platform of a micro-robotic micromanipulation system.

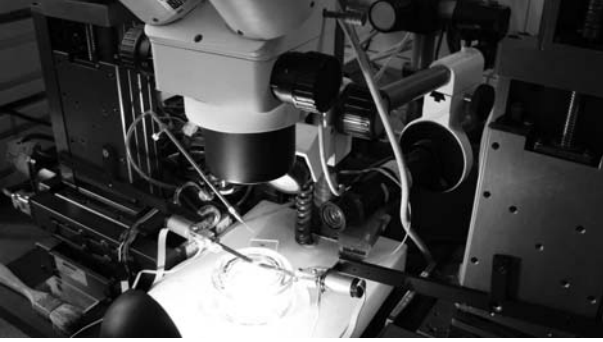
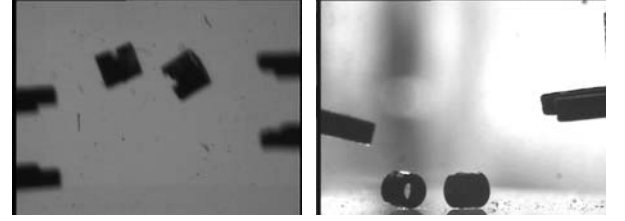


Fig. 2 The experiment platform of a robotic micromanipulation system

The experiment system consists of three parts. The first is a micro-moving platform, including three micro-manipulators. The second are micro-grippers, including two grippers driven by piezoelectricity and a vacuum adsorption micro-gripper. The third is a two-way orthogonal optical micro-vision platform, including a horizontal microscope and a vertical microscope.

5.1 Feature extraction

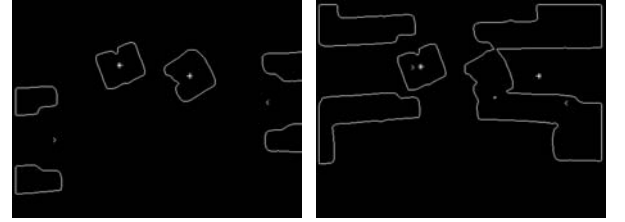
The main task of the experiment is to identify and classify the micro grippers and targets which can provide convenience for follow-up visual servoing task. Fig. 3 shows the original images of the targets and grippers in microscopic environment. Fig. 4 shows the extraction edges of the targets and grippers.



(a) Vertical view

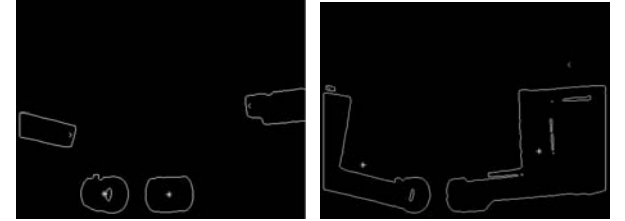
(b) Horizontal view

Fig. 3 Original microscopic images in vertical and horizontal view fields



(a) Vertical edges of targets

(b) Horizontal edges of targets



(c) Vertical edges of grippers

(d) Horizontal edges of grippers

Fig. 4 The extracted edges of the targets and grippers

5.2 Results of identification and analysis

Table 1 gives the normalized feature attribute values of the four different objectives using invariant moment algorithm. We compute the feature attributes of objects in all directions and only list the feature attributes in one direction.

We firstly compare the data classification effectiveness on a number of micro objects by using the traditional support vector machine algorithm and SVM + rough set. The results are shown in Table 2.

According to Table 2, the correction rate of classification based on the proposed SVM + rough set classification algorithm is 95.89%, which is higher than the single SVM algorithm correction rate (93.45%). So, it can be concluded here that the attribute reduction improves the classification ability. Besides, compared with the calculation time, it can be seen clearly from Table 2 that the calculation time of the proposed algorithm is about five times less than that of the single SVM algorithm so that the system becomes more effective in real time.

Table 1 The feature attribute normalization values of different objects using invariant moments algorithm

Category	F_1	F_2	F_3	F_4	F_5	F_6	F_7
Cylindrical part	1.0000	-0.9910	0.9935	-0.1600	0.1076	1.0000	-0.5762
Glass small ball	1.0000	0.9900	-0.9946	0.1822	0.1178	0.9952	-0.5486
Piezoelectricity gripper	-0.9897	-0.7610	-1.0000	-1.0000	-0.9999	0.9554	-1.0000
Vacuum gripper	0.1673	0.9993	0.3131	0.9915	0.9857	-0.9577	0.9861

Table 2 The comparison results of using two classification methods

SVM classification correction rate	Time (ms)	SVM + rough set classification correction rate	Time (ms)
93.45 %	2108.24	95.89 %	357.65

Table 3 The comparison results of classification accuracy

Serial number	Property	SVM classification accuracy	SVM + rough set classification accuracy
1	10	90.00 %	95.10 %
2	15	90.25 %	96.00 %
3	9	89.00 %	92.87 %
4	21	92.15 %	97.08 %
5	15	90.80 %	92.33 %
6	12	90.00 %	93.50 %
7	12	94.00 %	95.22 %
8	20	92.16 %	97.40 %

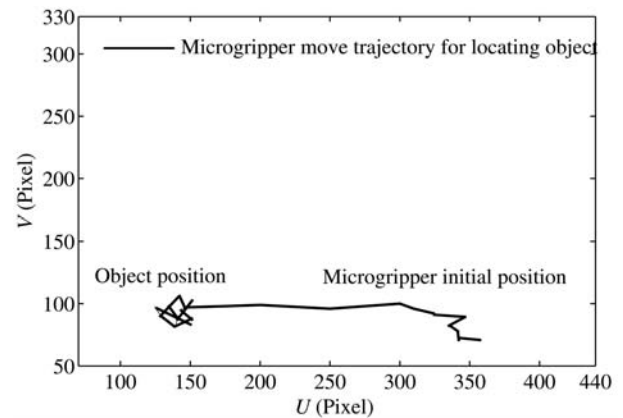
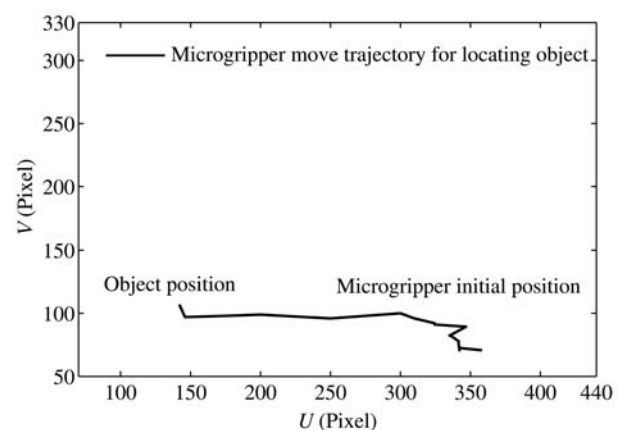
Table 3 provides the comparison results of classification accuracy using SVM classification and SVM + rough set classification for 25 feature attributes (gray, area, perimeter, texture, etc.). In Table 3, the first column is serial number of data sets; the second column is the number of conditions attributes after attribute reduction; the third column is classification accuracy with SVM; the fourth column is classification accuracy with SVM + rough set algorithm. The number of conditions attributes of the final classification for entering to SVM is 14.25, less than 25 feature attributes. This simplifies the follow-up SVM forecast classification process.

5.3 Positioning test

To accomplish micromanipulator positioning and gripping micro-parts, the centers of objects and grippers should be obtained first. The centers can be accessed by a series of image processing, including graying, denoising, filtering, canny operating, edge extraction, fuzzy c -means clustering, and so on. In Fig. 4, the X - Y image plane coordinates of the object center are (147, 99) and the gripper center (343, 77).

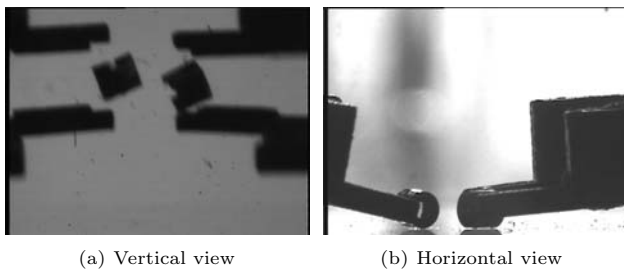
Assume that the initial parameters of PD controller K_p and K_d are 10 and 0, respectively, which means that the system is only joined proportional control. The control effect is shown in Fig. 5. We can see that the implementation of automatic positioning objects to the target center has biggish oscillation and overshoot. When $K_p = 10$ and $K_d = 1.5$, the proportional and differential controls are incorporated. The control result is shown in Fig. 6.

The joined differential item inhibits the system overshoot, and the system meets the rapidity and smoothness. Finally, the implementation of micro-manipulator positioning and automatic gripping operations is given. The satisfied implementation can be obtained with the results to meet the system application requirements. Fig. 7 shows the image of the end effector automatically locating object.

Fig. 5 The trajectory of micromanipulator approaching goal object with only proportional control (X - Y plane)Fig. 6 The trajectory of micromanipulator approaching goal objects with proportional and differential control (X - Y plane)

Finally, we give the comparison results of the convergence speed of the cost function based on Chebyshev polynomials and RLS, as shown in Fig. 8. It is clear from Fig. 8 that the cost function based on Chebyshev polynomials improves the

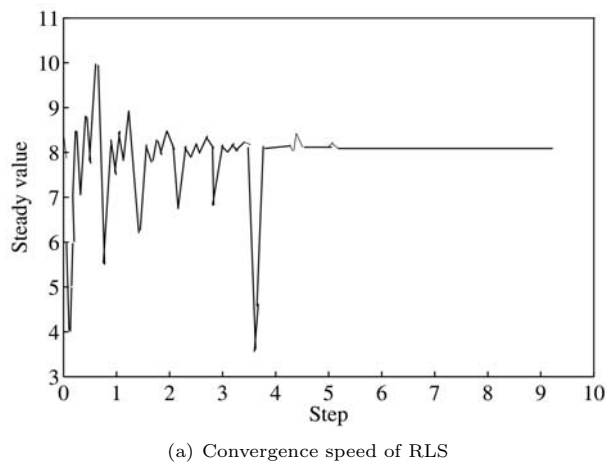
system identification process of convergence compared with the RLS algorithm.



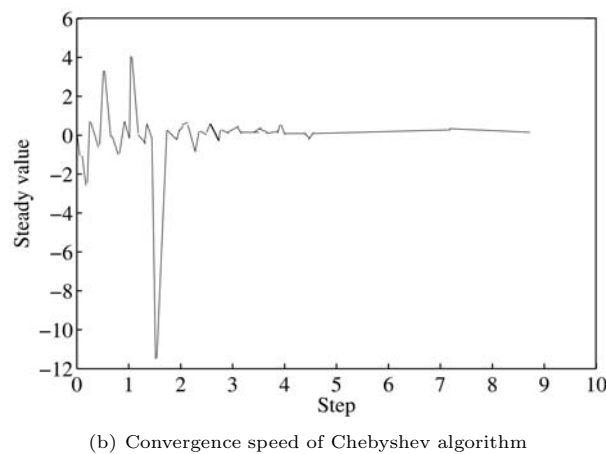
(a) Vertical view

(b) Horizontal view

Fig. 7 The images of end effectors automatically locating and gripping objects in vertical and horizontal view fields



(a) Convergence speed of RLS



(b) Convergence speed of Chebyshev algorithm

Fig. 8 The comparison results of the convergence speeds

6 Conclusions

In a 3D micro-size robotic assembly system, an improved support vector machine algorithm is presented, which is used to identify multiple micro objects. An improved Broyden's method is proposed to estimate the image Jacobian matrix online which employs Chebyshev polynomial to construct a cost function to approximate the optimization value. Finally, a PD controller is designed for the micro-manipulator. In the microscopic visual environment, the proposed methods are used to complete visual servoing

tasks of a micromanipulator with positioning and automatically gripping micro-parts. The experimental results show that the proposed methods and algorithm are effective.

References

- [1] M. K. Hu. Visual attribute recognition by moment invariants. *IEEE Transactions on Information Theory*, vol. 8, pp. 179–187, 1962.
- [2] E. Bermiani, A. Boni, S. Caorsi, A. Massa. An innovative real time technique for buried object detection. *IEEE Transactions on Geoscience and Remote Sensing*, vol. 41, no. 4, pp. 927–931, 2003.
- [3] L. R. Jose, M. Manel, D. P. Mario. Support vector method for robot ARMA system identification. *IEEE Transactions on Signal Processing*, vol. 52, no. 1, pp. 155–164, 2004.
- [4] Y. Chen, J. Z. Wang. Support vector learning for fuzzy rule based classification systems. *IEEE Transactions on Fuzzy System*, vol. 11, no. 6, pp. 716–727, 2003.
- [5] J. Peng, D. R. Heisterkamp, H. K. Dai. LDA/SVM driven nearest neighbor classification. *IEEE Transactions on Neural Networks*, vol. 14, no. 4, pp. 940–942, 2003.
- [6] A. H. Sung, S. Mukkamala. Identifying important features for intrusion detection using support vector machines and neural networks. In *Proceedings of Symposium on Applications and the Internet*, IEEE, pp. 209–216, 2003.
- [7] D. Kaibo, S. S. Keerthi, N. P. Aun. Evaluation of simple performance measures for tuning SVM hyperparameters. *Neurocomputing*, vol. 51, no. 1, pp. 41–59, 2003.
- [8] J. Liu, D. Li, W. Tao, L. Yan. An automatic method for generating affine moment invariants. *Pattern Recognition Letters*, vol. 28, no. 16, pp. 2295–2304, 2007.
- [9] R. Jensen, Q. Shen. Fuzzy rough sets assisted attribute selection. *IEEE Transactions on Fuzzy Systems*, vol. 15, no. 1, pp. 73–89, 2007.
- [10] C. R. Yu, H. W. Wang, Y. Luo. A heuristic algorithm for attribute reduction of decision making problem based on rough set. In *Proceedings of the 6th International Conference on Intelligent Systems Design and Applications*, IEEE, vol. 1, pp. 503–508, 2006.
- [11] Q. S. Kang, T. Hao, Z. D. Meng, X. Z. Dai. Pseudo inverse estimation of image Jacobian matrix in uncalibration visual servoing. In *Proceedings of IEEE International Conference on Mechatronics and Automation*, IEEE, pp. 1515–1520, 2006.
- [12] A. S. Malik, T. S. Choi. Consideration of illumination effects and optimization of window size for accurate calculation of depth map for 3D shape recovery. *Pattern Recognition*, vol. 40, no. 1, pp. 154–170, 2007.
- [13] Y. Shen, D. Sun, Y. H. Liu, K. Li. Asymptotic trajectory tracking of manipulators using uncalibrated visual feedback. *IEEE/ASME Transactions on Mechatronics*, vol. 8, no. 1, pp. 87–98, 2003.

- [14] J. A. Piepmeyer, G. V. MacMurray, H. Lipkin. A dynamic quasi-Newton method for uncalibrated visual servoing. In *Proceedings of IEEE International Conference on Robotics and Automation*, IEEE, Detroit, MI, USA, vol. 2, pp. 1595–1600, 1999.
- [15] J. A. Piepmeyer, G. V. MacMurray, H. Lipkin. Uncalibrated dynamic visual servoing. *IEEE Transactions on Robotics and Automation*, vol. 20, no. 1, pp. 143–147, 2004.
- [16] E. Malis. Visual servoing invariant to changes in camera-intrinsic parameters. *IEEE Transactions on Robotics and Automation*, vol. 20, no. 1, pp. 72–81, 2004.
- [17] J. Su, H. Ma, W. Qiu, Y. Xi. Task-independent robotic un-calibrated hand-eye coordination based on the extended state observer. *IEEE Transactions on Systems, Man, and Cybernetics — Part B: Cybernetics*, vol. 34, no. 4, pp. 1917–1922, 2004.
- [18] S. Hutchinson, G. D. Hager, P. I. Corke. A tutorial on visual servo control. *IEEE Transactions on Robotics and Automation*, vol. 12, no. 5, pp. 651–670, 1996.
- [19] Q. Shen, R. Jensen. Rough sets, their extensions and applications. *International Journal of Automation and Computing*, vol. 4, no. 3, pp. 217–228, 2007.
- [20] C. Bean, C. Kambhampati. Autonomous clustering using rough set theory. *International Journal of Automation and Computing*, vol. 5, no. 1, pp. 90–102, 2008.
- [21] A. Skowron, C. Rauszer. The discernibility matrices and functions in information systems. *Intelligent Decision Support-handbook of Applications and Advances of the Rough Sets Theory*, R. Slowinski, Ed., Kluwer Academic Publishers, pp. 331–362, 1992.



Xin-Han Huang graduated from Huazhong University of Science and Technology (HUST), Wuhan, PRC in 1969. He worked at the Robotics Institute of Carnegie-Mellon University, Pittsburgh, USA, as a visiting scholar from 1985 to 1986 and the Systems Engineering Division of Wales University, Cardiff, UK, as a senior visiting scholar in 1996. He is currently a professor and head of the Intelligence and

Control Engineering Division of HUST. He is a senior member of the Chinese Automation Society and chairman of the Intelligent Robot Specialty Committee of the Chinese Association for Artificial Intelligence (CAAI).

His research interests include robotics, sensing techniques, data fusion, and intelligent control.

E-mail: xhhuang@mail.hust.edu.cn (Corresponding author)



Xiang-Jin Zeng received his B. Eng. degree in 2000 and M. Eng. degree in 2006, both from Huazhong University of Science and Technology (HUST), Wuhan, PRC. Since 2006, he has been a Ph. D. candidate of HUST, majoring in control science and engineering.

His research interests include microscope visual servoing, image procession, robotics, and embedded system.

E-mail: xjzeng21@163.com



Min Wang received B. Eng. and M. Eng. degrees from Huazhong University of Science and Technology (HUST), Wuhan, PRC in 1982 and 1989, respectively. She is currently a professor of the Department of Control Science and Engineering of HUST. She is a secretary-general of the Intelligent Robots Specialty Committee of the Chinese Association for Artificial Intelligence (CAAI).

Her research interests include robotics, sensing techniques, neural networks and their applications.

E-mail: wm526@163.com